UC San Diego

UC San Diego Previously Published Works

Title

Repositioning the Early Pathology of Type 1 Diabetes to the Extraislet Vasculature.

Permalink

https://escholarship.org/uc/item/8dc76361

Journal

Journal of Immunology, 212(7)

Authors

Costanzo, Anne

Clarke, Don

Holt, Marie

et al.

Publication Date

2024-04-01

DOI

10.4049/jimmunol.2300769

Peer reviewed

eScholarship.org Powered by the California Digital Library
University of California

Repositioning the Early Pathology of Type 1 Diabetes to the Extraislet Vasculature

Anne Costanzo,* Don Clarke,* Marie Holt,* Siddhartha Sharma,* Kenna Nagy,* Xuqian Tan,† Lisa Kain,* Brian Abe,* Sandrine Luce,‡ Christian Boitard,‡ Tine Wyseure,§ Laurent O. Mosnier,§ Andrew I. Su,† Catherine Grimes,¶ M. G. Finn,‖ Paul B. Savage,# Michael Gottschalk, Jeremy Pettus,†† and Luc Teyton***

Type 1 diabetes (T1D) is a prototypic T cell–mediated autoimmune disease. Because the islets of Langerhans are insulated from blood vessels by a double basement membrane and lack detectable lymphatic drainage, interactions between endocrine and circulating T cells are not permitted. Thus, we hypothesized that initiation and progression of anti-islet immunity required islet neolymphangiogenesis to allow T cell access to the islet. Combining microscopy and single cell approaches, the timing of this phenomenon in mice was situated between 5 and 8 wk of age when activated anti-insulin CD4 T cells became detectable in peripheral blood while peri-islet pathology developed. This "peri-insulitis," dominated by CD4 T cells, respected the islet basement membrane and was limited on the outside by lymphatic endothelial cells that gave it the attributes of a tertiary lymphoid structure. As in most tissues, lymphangiogenesis seemed to be secondary to local segmental endothelial inflammation at the collecting postcapillary venule. In addition to classic markers of inflammation such as CD29, V-CAM, and NOS, MHC class II molecules were expressed by nonhematopoietic cells in the same location both in mouse and human islets. This CD45$^-$ MHC class II$^+$ cell population was capable of spontaneously presenting islet Ags to CD4 T cells. Altogether, these observations favor an alternative model for the initiation of T1D, outside of the islet, in which a vascular-associated cell appears to be an important MHC class II–expressing and –presenting cell. ***The Journal of Immunology*****, 2024, 212: 1094–1104.**

One striking feature of the pathology of type 1 diabetes (T1D) is the asynchrony of islet lesions. In prediabetic NOD mice and humans, it is frequent to see side-by-side healthy islets, islets surrounded by immunocytes, islets undergoing destruction, and islets that have lost all β cells (1, 2). This feature is likely indicative of the normal physiology of the endocrine pancreas in which each islet operates individually and can be sacrificed without altering function. This uncoordinated strategy could also explain why the destruction of 1.5 g of tissue in humans is slow and takes 5 y on average (3), following a relapse–remission pattern similar to most other autoimmune diseases (4). We have recently shown that the 15–20% nondiabetic mice in our colony had had disease but enough residual islets to be normoglycemic (5). These considerations about progression are critical to diagnose islet autoimmunity early and time potential preclinical therapeutic interventions (5).

It has been shown that CD4 and CD8 T cells were important for disease onset and progression, respectively (6, 7). From the immunological standpoint, β cells could be killed directly by CD8 T cells, or indirectly by immune cytokine stress (8). Although many islet Ags have been discovered, their processing and presentation remain a debated issue (9, 10). The nature of APCs is even more controversial. For CD8 killing it has been consistently shown that β cells express MHC class I molecules, especially after cytokine exposure (11); however, their ability to synthesize and display MHC class II is not a closed issue (12). Some studies have shown expression of MHC class II by β cells upon stimulation by T cell cytokines (13), or in vivo (14, 15), but never early during disease progression and/or by a large number of cells (12, 15). Other studies have shown that only hematopoietic cells present in the islet could express MHC class II (16). If the β cell is not the main APC for initiating CD4

*Department of Immunology and Microbiology, The Scripps Research Institute, La Jolla, CA; †Department of Integrative Structural and Computational Biology, The Scripps Research Institute, La Jolla, CA; ‡INSERM U1016, Institut Cochin, Paris, France; §Department of Molecular Medicine, The Scripps Research Institute, La Jolla, CA; ¶Department of Chemistry and Biochemistry, University of Delaware, Newark, DE; ‖School of Chemistry and Biochemistry, Georgia Institute of Technology, Atlanta, GA; #Department of Chemistry and Biochemistry, Brigham Young University, Provo, UT; **Rady Children's Hospital, University of California San Diego, San Diego, CA; and ††UC San Diego School of Medicine, University of California San Diego, San Diego, CA

ORCIDs: 0000-0003-1917-1566 (D.C.); 0000-0003-0763-4535 (M.H.); 0000-0002-3772-3160 (K.N.); 0000-0001-5873-8647 (L.K.); 0000-0002-1262-5556 (B.A.); 0000-0002-9519-333X (S.L.); 0000-0003-2337-3443 (T.W.); 0000-0003-1195-964X (L.O.M.); 0000-0002-9859-4104 (A.I.S.); 0000-0001-8247-3108 (M.G.F.); 0000-0002-5214-9929 (M.G.); 0000-0002-5999-0091 (J.P.).

Received for publication November 9, 2023. Accepted for publication January 29, 2024.

This work was supported by grants from the National Institutes of Health, including a Clinical and Translational Science Award issued to the Scripps Translational Science Institute through National Center for Advancing Translational Sciences Grants UL1TR002550 and TL1TR002551 (to S.S., D.C., and K.N.), KL2TR001112 (to B.A.), National Heart, Lung, and Blood Institute Grant 1 R01HL148096 (to L.O.M.), Division of Diabetes, Endocrinology, and Metabolic Diseases Grant 1R01DK117138 (to L.T., M.G., and J.P.), and Division of Microbiology and Infectious Diseases Grant 1R01 AI139748 (to L.T., M.G.F., and P.B.S.). nPOD (RRID:SCR_014641) is a collaborative type 1 diabetes research project supported by JDRF (nPOD: 5-SRA-2018-557-Q-R) and by The Leona M. & Harry B. Helmsley Charitable Trust (Grant 2018PG-T1D053, G-2108-04793).

The single-cell data presented in this article have been submitted to the Gene Expression Omnibus (https://www.ncbi.nlm.nih.gov/geo/query/acc.cgi?acc=GSE253956) under accession number GSE253956.

Address correspondence and reprint requests to Dr. Luc Teyton, Scripps Research Institute, 10550 North Torrey Pines Road, IMM 23, Room 301, La Jolla, CA 92037. E-mail address: lteyton@scripps.edu

The online version of this article contains supplemental material.

Abbreviations used in this article: BM, basement membrane; IATLS, islet-associated TLS; MDP, muramyl dipeptide; NOS3, NO synthase 3; nPOD, Network for Pancreatic Organ Donors with Diabetes; pLN, peripheral lymph node; poly(I:C), polyinosinic-polycytidylic acid; T1D, type 1 diabetes; TLS, tertiary lymphoid structure.

This article is distributed under The American Association of Immunologists, Inc., Reuse Terms and Conditions for Author Choice articles.

Copyright © 2024 by The American Association of Immunologists, Inc. 0022-1767/24/$37.50

https://doi.org/10.4049/jimmunol.2300769

T cells, what cells are performing this function? The intraislet macrophage has that capacity (17), but because CD4 T cells are not found next to it, it is difficult to qualify the early diabetic lesion as "T cell infiltration." When CD4 T cells and HLA-DR$^+$ cells are visualized as in the original description of an immune lesion associated with T1D by Bottazzo et al. (18), the cells are all localized at the periphery of the islet, not within. This observation has been confirmed since in numerous studies examining the pathology of T1D islets (19–21). Thus, it is logical to posit that neither the intraislet macrophage nor the β cell is the initiating APC.

This quest for other MHC class II$^+$ cells associated with the islet became a priority after we determined that opposite to other Ags (22), the site of polyclonal anti-insulin CD4 T cell priming and activation in mouse T1D was the islet and not the draining lymph node (23), confirming results from transgenic TCR mice (24). This finding was all the more surprising given the absence of detectable lymphatic drainage for both normal rodent and human islets (25), a feature that endows islets with the rare status of an "immune privileged site." In this study, the examination of the activation of circulating anti-insulin CD4 T cells in peripheral blood of NOD mice assigned the timing of recirculation from the islet, thus the presence of islet-associated lymphatics, between weeks 5 and 8, a window that also corresponded to the appearance of islet pathology. Immunocytochemistry was used to show that the building of tertiary lymphoid structures (TLSs) happened outside of the islet basement membrane (BM) (26). Most interestingly, islet-associated TLSs (IATLSs) seemed to originate and grow near the efferent vascular bundle of each individual islet, suggesting that disease initiation might be linked to unique features of these blood vessels (27). As a reminder, both in mice and humans, islets usually have a single artery, sometimes two, and four to seven efferent postcapillary venules that collect a dense capillary bed (28–30).

The vasculature of the islet was examined at steady state and after immunological challenges applied to the duodenum for stigma of inflammation, the most common trigger of lymphangiogenesis (31, 32). In normal conditions, sporadic evidence of endothelial activation was noted on segments of the vasculature, including the proximal collecting venules of the islet. This "normal" chronic exposure of the pancreatic vasculature to inflammatory cues on a genetic at-risk background could trigger disease by allowing T cell arrest and extravasation; the influx of hematopoietic cells would then promote lymphangiogenesis (33). Such a scenario was supported by the recurrence of disease progression in each of four therapeutic interventions that targeted key cells or molecules involved in lymphangiogenesis. In addition, a population of nonhematopoietic MHC class II$^+$ cells that is integral to the IATLS was shown to spontaneously present Ags to CD4 T cells and might be the "missing" APC that initiates pathology.

Materials and Methods

Mice

NOD/LtJ mice were purchased from The Jackson Laboratory and housed in pathogen-free conditions. House-bred NOD/LtJ 57D, NOD/LtJ H2A$^{-/-}$, and C57Bl6-I-A^{g7} mice were also used in this study. YES mice, humanized by transgenesis with HLA-A201, HLA-DQ0302, and human insulin in an MHC class I and class II knockout background (34), were kept at the Cochin Institute (Paris) under pathogen-free conditions. For histology, all mice used in this study were females between the age of 5 and 10 wk to allow easier comparison; ~450 animals were necessary to perform at least two separate experiments in which two to four animals for each combination of Abs were examined. Another ~200 animals were used for longitudinal studies (Fig. 1) and therapeutic interventions (Fig. 4). Care and handling of mice followed Institutional Animal Care and Use Committee rules.

Human tissues

Normal human and diabetic pancreatic tissues were obtained from the Network for Pancreatic Organ Donors with Diabetes (nPOD) program and MyBiosource. T1D donors were nPOD ID nos. 6209, 6228, 6247, 6362, 6380, 6399, 6414, 6520, 6523, and 6526. Normal donors were nPOD nos. 6468, 6516, 6525, and samples from MyBiosource.

Longitudinal blocking/survival studies

Axitinib was injected i.p. every other day for 14 d (25 mg/kg in a volume of 100 μl) (Cayman Chemical). Sodium acetate was injected i.p. every day for 3 wk at a dose of 400 μl of 0.5 M stock solution. mAbs were injected i.p. once a week for 3 consecutive weeks at a dose of 200 μg per mouse. Control groups were injected with DMSO in small-molecule experiments and isotype control Abs in Ab experiments. Glycemia was measured weekly for 25 wk from blood collected from the tip of tail; mice were considered diabetic when blood glucose was ≥250 mg/dl for 2 consecutive weeks. Statistical evaluation was performed using Prism software. For survival, the log rank/Mantel–Cox test was used for blood glucose, and a mixed effects analysis was used to evaluate the differences during the course of the entire experiment. Finally, hazard ratios were calculated as the Mantel–Haenszel statistic/slope of the survival curve.

Gavage

Polyinosinic-polycytidylic acid (poly(I:C); InvivoGen) was orally gavaged at a dose of 100 μg per mouse after mixing in equal parts with olive oil and heavy cream in a final volume of 100 μl. Pancreas/duodenum blocks were excised and embedded in OCT compound. Tissues were stored at −80°C until sectioning. In all gavage experiments, control groups received only the olive oil and heavy cream mix.

Islet isolation and cell preparation

Islets were isolated using a modified protocol derived from Li et al. (35). Briefly, pancreases were perfused with 0.5 mg/ml collagenase P (Sigma-Aldrich, 11213865001) through the common bile duct and digested at 37°C for 17 min. After several washes, pancreatic slurry was passed through a 0.419-mm wire mesh strainer. A density gradient was established by layering Histopaque-1077 (Sigma-Aldrich) and serum-free RPMI 1640, and sample was loaded on top. After centrifugation at 400 × *g* for 20 min, islets were collected at the Histopaque/media interface, washed, and hand-picked under a dissecting microscope. An average of 300–400 islets were recovered per mouse. For making single-cell suspensions, islets were digested with trypsin-EDTA and washed extensively before being counted.

Cell staining and flow cytometry analysis and sorting

Islet single-cell suspensions were washed with FACS buffer (PBS containing 3% FCS and 0.05% NaN_3) and incubated in Fc Block (BD Biosciences) for 15 min at room temperature. Cells were then stained with the appropriate mixture of Abs and peptide-MHC tetramers as previously described (23). In every experiment, a fluorescence minus one control was included for each Ab. Flow cytometry was performed using a MACSQuant analyzer (Miltenyi Biotec) and data were analyzed using FlowJo software (Tree Star). Single-cell sorting was performed on a Becton Dickinson FACSAria III machine at the Scripps Core Facility. All Abs were used according to the manufacturers' recommendations for species specificity and dilution.

T cell assays

A NFAT ametrine biosensor cloned into the transposon vector pT4/HB (Addgene, plasmid no. 108352) was transfected in BDC2.5 T cell hybridoma. Clones were established after puromycin selection. Activation of the cells (4×10^4) was measured at 16 h postchallenge with APCs (dissociated islets) by flow cytometry; the NFAT-mAmetrine signal was excited at 405 nm, and emission was collected in the VioGreen channel of a MACSQuant analyzer. CD45 depletion was performed using a double pass on CD45 microbead mouse columns (Miltenyi Biotec). Efficiency was confirmed by flow cytometry and was >95%.

Single-cell analysis

For single-cell analysis, cells were sorted directly into RT buffer (5 μl per well). Protocols for preamplification and amplification for gene expression analysis and TCR sequencing have been detailed in recent publications (23, 36). The list of genes used to profile macrophages and endothelial cells is shown in Supplemental Fig. 2. Single-cell quantitative PCR was run on a Fluidigm BioMark suite of instruments following the manufacturer's instructions. Data analysis used the manufacturer's software and in-laboratory R scripts that have been published (23).

Abs and immunofluorescence staining of frozen sections

All human samples were provided as slides from fresh-frozen sections (10 μm thickness). Mouse pancreases were excised and embedded in OCT compound. Tissue was sectioned at 7 μm and fixed using 4% paraformaldehyde for 15 min. After washing several times with PBS, tissue was permeabilized using 0.2% Triton X-100 (15 min) and blocked in 5% normal goat serum/5% fish gelatin for 30 min. Primary Abs (see Supplemental Table I) were diluted in blocking buffer and incubated from 2 h–overnight at 4°C. Anti-CD3 Abs were produced in-house (2C11 and 500A2), anti-CD4 Abs were from BD Biosciences and Abcam, and anti-CD8 was from Abcam. Sections were washed and incubated in secondary Ab at room temperature for 40 min–1 h. Hoechst DAPI solution was used for nuclear counterstains. All Abs were used according to the manufacturers' recommendations for species specificity and dilution. All costainings were carried out sequentially. Images were acquired using a Zeiss 780 confocal microscope using oil immersion objectives of 10, 20, and ×63 magnification.

To be representative, for each Ab, images were obtained from at least two independent experiments and from two to four animals in each experiment. All experiments including a secondary control Ab were run with the secondary Ab alone to avoid nonspecific background and to set up the threshold using the fluorescence minus one approach (for each wavelength, autofluorescence from unstained and secondary Abs alone were examined to set up threshold and remove background). Acquisition parameters were never modified between samples examined with the same combination of fluorophores.

Production of anti–muramyl dipeptide Abs

A synthetic form of muramyl dipeptide (MDP) was modified at the anomeric position, yielding a clickable linker through neoglycosylation chemistry and coupled to modified bacteriophage yielding an immunization particle as previously described (37). Then, 100 μg of particle and 500 ng of PBS-57 as adjuvant were delivered i.m. at week 0 and 6 to C57BL/6 mice (6–8 wk of age), and mice were boosted i.v. 3 d before euthanasia. Harvested spleens were fused to myelomas (P3X63Ag8.653) with HAT (hypoxanthine, aminopterin, and thymidine) selection media to isolate hybridomas; specificity was confirmed using ELISA and surface plasmon resonance on MDP-coated surfaces and a series of bacterial glycans as control. Anti-LPS Abs were from commercial sources (Thermo Fisher Scientific and LS Bio).

Data and resource availability

All single-cell data have been deposited and are accessible at the Gene Expression Omnibus (National Center for Biotechnology Information) under accession number GSE253956 (https://www.ncbi.nlm.nih.gov/geo).

Results

Detection and phenotype of insulin-specific CD4 T cells in peripheral blood

Insulin-specific cells were enumerated weekly from 3 to 12 wk in the peripheral blood of unmanipulated NOD mice using register-specific insulin peptide I-A^{g7} tetramers (23); this experiment was performed without magnetic enrichment, as this step only marginally improved efficiency while reducing cell viability (Fig. 1A, 1B). Following an early peak at weaning, numbers for both $Ins_{12–20}$ and $Ins_{13–21}$ I-A^{g7} tetramers leveled down at ∼0.2% of total CD4 T cells and then showed two bursts at 6 and 10 wk. More importantly, when activation was profiled at the single-cell level with a battery of 96 genes (23), it appeared that although cells were quiescent at week 5, ∼70% of them were activated at week 8 (Fig. 1C), with a profile very closely related to the one of islet-infiltrating CD4 T cells with differential expression of genes such as IL-2Ra, ICOS, IFN-γ, and TNF-α (Fig. 1D) (23). This observation was suggestive that the activated cells were originating from islets, and fitted well with the pathology observed in NOD mice, that is, normal islets with no detectable lymphatics (38, 39) until weeks 4–6, followed by microscopic pathology around weeks 6–8 (40, 41).

Circulation of pathogenic, islet-specific CD4 T cells in the NOD mouse model

Although the transfer of splenocytes has been shown to confer disease (42), and islet Ag-specific T cells have been isolated from peripheral blood (43), the capacity of circulating cells to initiate disease has not yet been supported experimentally. To directly address this paradigm, pairs of 3-wk-old CD45.1 and CD45.2 allotypically labeled NOD mice were parabiosed. After 3–4 wk postsurgery, 6 out of 10 pairs were sacrificed and bulk CD4 T cell exchange was assessed in multiple tissues. In all pairs, near equal exchange between CD45.1 and CD45.2 CD4 T cells in spleen, peripheral blood, and islets was observed (Supplemental Fig. 1A).

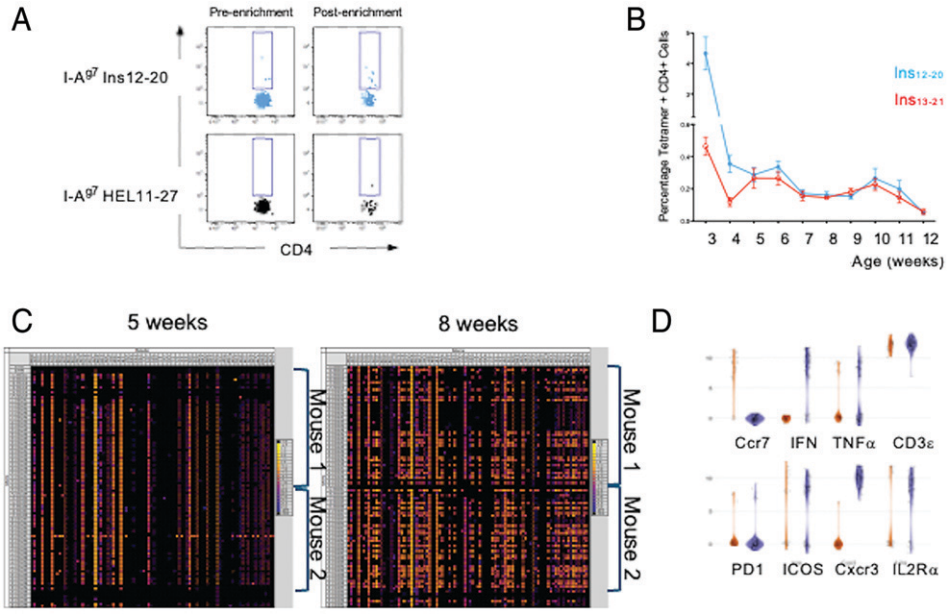

FIGURE 1. Detection of $Ins_{12–20}$- and $Ins_{13–21}$-reactive T cells in peripheral blood of NOD mice. (**A**) Typical example of a I-$A^{g7}Ins_{12–20}$ tetramer staining on peripheral blood with or without magnetic enrichment. The $HEL_{11–27}$ peptide was used as a control. (**B**) Time course of I-$A^{g7}Ins_{13–21}$ and I-$A^{g7}Ins_{12–20}$ tetramer CD4-positive T cells in peripheral blood from 3 to 12 wk of age (five mice in this experiment). (**C**) Heatmap of $Ins_{12–20}$ (top 24 cells for each mouse) and $Ins_{13–21}$ (bottom 24 cells for each mouse) tetramer-positive cells in two mice sampled at weeks 5 and 8. Columns are genes, rows are individual cells. (**D**) Violin representation of the top differentially expressed genes found in dormant (brown) versus activated cells (blue) at week 8 in the mice presented in (C).

To test the pathogenicity of the circulating cells, parabioses between NOD and immunocompromised NOD-SCID mice were established. In five out of five pairs, both mice were diabetic at 20 wk. The pathology of the NOD-SCID pancreas of three additional pairs confirmed peri-islet infiltration of CD4 T cells (Supplemental Fig. 1B).

Thus, we concluded that pathogenic autoimmune CD4 T cells recirculated and could access the pancreatic islets. This observation needed to be put in the context of two important physiopathology features of the endocrine pancreas: islets do not have an autonomous lymphatic drainage (25), and in the preclinical phase of T1D, insulin-specific CD4 T cells receive TCR-mediated activation in islets, not the main peripheral lymph nodes (pLNs) (23). This latter point was reinforced by an experiment that complemented the parabiotic study and consisted of removing the main pLN from either or both animals before parabiosis (Supplemental Fig. 1C). Three weeks after surgery, 6 out of 10 pairs were sacrificed and bulk CD4 T cell exchange was assessed in tissues. In all pairs, a near equal exchange between CD45.1 and CD45.2 CD4 T cells in spleen, peripheral blood, and islets was observed (Supplemental Fig. 1C), and pLN removal from either or both animals did not affect this distribution.

These observations reinforced the notion that in preclinical NOD mice T cell priming happens in association with the islet and not in the main pLN (23, 24) and confirmed that at steady state there is no communication of the islet with the lymphatic system. However, the appearance of activated circulating CD4 T cells in peripheral blood at 8 wk of age indicated that disease progression was associated with a communication with the lymphatic circulation. Therefore, we hypothesized that the islet-associated lesion designated as insulitis for the past three decades corresponded to the construction of lymphatic structures capable of enabling communication between islets and lymph nodes, and the subsequent recirculation of lymphocytes from damaged islets.

Islet pathology corresponds to the construction of a tertiary lymphoid structure

The pathology of immune-privileged organs undergoing autoimmune attack has revealed the presence of TLSs associated with lesions in all species (44–46); some of these, when persistent in time, resemble lymph nodes with T and B cell zones and are called tertiary lymphoid organs (47). In this study, TLSs are defined as structures limited by a lymphatic endothelium stained by LYVE-1 or podoplanin. How lymphangiogenesis establishes TLSs and tertiary lymphoid organs in autoimmunity is still poorly understood (47), but inflammation is believed to be its driver (32, 48, 49).

Lymphangiogenesis associated with the islet of Langerhans was examined in 5- to 9-wk-old NOD mice. Lymphatic structures were stained with two classic markers of lymphatic endothelium, anti–LYVE-1 and anti-podoplanin Abs, whereas islets were visualized for insulin expression (Fig. 2). This examination confirmed the absence of detectable lymphatics in normal mouse and human islets (Fig. 2A; see Fig. 6A) while revealing the presence of lymphatics as soon as CD4 T cell infiltration was present (Fig. 2B–D). IATLS draining lymphatics connected to the exocrine pancreas lymphatic vasculature (Fig. 2C, 2D). In all cases, the early lesion was localized next to efferent blood vessels and outside of the islet; given that most neolymphatics differentiate from veins (50), this feature was expected (Fig. 2C, 2D). A closer view of this early lesion showed that IATLSs were overwhelmingly filled with $CD4^+$ T cells whereas $CD8^+$ T cells were rare (7) (Fig. 2E, 2F). In no section, LYVE-1 staining could identify valves in the conduits leaving from IATLSs. Out of 34 islets with associated insulitis examined for insulin/LYVE-1 staining, 33 islets had associated expression of LYVE-1 on the outside of the insulitis and a single one did not. None of the 53 islets without lesion present in the same set of slides exhibited LYVE-1 expression.

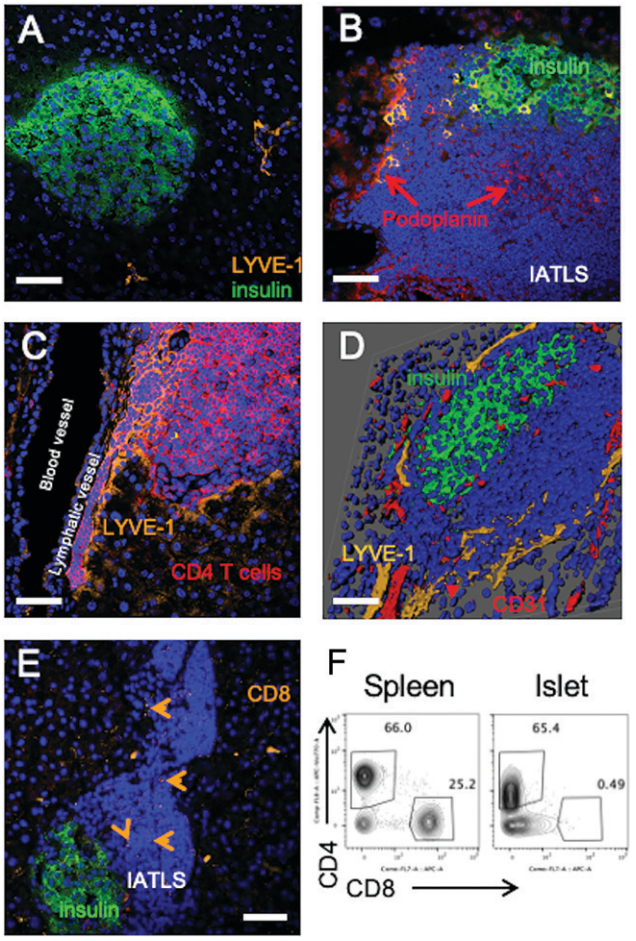

FIGURE 2. Formation of juxta-islet tertiary lymphoid structures during the progression of diabetes in NOD mice. (**A**) No lymphatics were detected in association with normal islets. (**B**) Podoplanin-expressing cells were present on the outside and inside the tertiary lymphoid structure that constituted the insulitis lesion. (**C**) Tertiary lymphoid structure were filled with $CD4^+$ T cells that drained into neolymphatics associated with normal venules. (**D**) Three-dimensional rendering of a typical tertiary lymphoid structure surrounding an islet. The outsides were limited by LYVE-1^+ cells, forming a sac that drained into a lymphatic associated with a $CD31^+$ blood vessel. (**E** and **F**) CD8 T cells were rare within early IATLs as shown at 9 wk of age NOD mice by immunodetection (E) and flow cytometry of cells recovered from dissociated islets (F). Spleen was used as a control (percentages out of the CD3 gate are presented). Scale bars, 50 μm.

IATLSs were scaffolded by ER-$TR7^+$ cells, a classical marker of stromal fibers, BM, and follicular reticular cells (51–53) (Supplemental Table I). ER-TR7 was also expressed by exocrine pancreatic trabecular cells, as well as by a layer of cells that limited the outside of the islets and intraislet vascular columns. Heparan sulfate–rich BMs had a nearly identical distribution (Supplemental Table I), but laminin 2, rich in islet BMs (54), was absent from IATLSs (Supplemental Table I). Based on these two markers, ER-TR7 and heparan sulfate, IATLSs were clearly insulated from the islet by BMs, but the respective composition of those BMs was different in islets and IATLSs.

A large survey of the critical factors that drive or are associated with lymphangiogenesis (32, 55) was undertaken. Cells (macrophages, platelets, neutrophils), extracellular matrix proteins, cell adhesion and guidance factors, vascular markers, soluble factors and receptors, transcription factors, and markers of inflammation were examined

by indirect immunofluorescence in mouse and human tissues (see Supplemental Table I). Some prominent molecules (32) are shown in Fig. 3 with Prox1, the key transcription factor of lymphangiogenesis, VEGF-C, the principal growth factor for lymphatics, and midkine, one of the important seeding molecules for lymphatic sprouting (56). All three were expressed by lymphatic endothelial cells associated with the efferent vessels of the IATLSs (Fig. 3). Otherwise, IATLSs were similar to all TLSs described to date with an increased expression of adhesion molecules such as NRP2, and the presence of MECA-79$^+$ high endothelial venules to facilitate the recirculation of IATLS lymphocytes (57) (Supplemental Table I).

Because macrophages are central to islet biology (17) and potential contributors to lymphangiogenesis (48, 58), F4-80$^+$ cells were examined by immunostaining and single-cell RNA quantitative PCR for the expression of Prox1 (Supplemental Fig. 2A). Only a small percentage of macrophages (~5%) expressed this transcription factor, but protein was produced and sometimes found translocated to the nucleus (Supplemental Fig. 2B). The targeted RNA interrogation of the islet macrophages (59) also revealed the expression of important chemokines for lymphangiogenesis such as CCL21 (60), and seeding factors for lymphatic sprouts, namely midkine (56) and SELENOP (61). T cell chemoattractants such as CXCL9 (62) and the enzymatic duo for S1P synthesis, S1P kinase and S1P lyase, were also detected (63). In conclusion, while some contribution of the macrophage was likely, it did not seem to dominate the biology of IATLSs.

IATLSs and progression of disease

The relevance of the IATLS organization to the pathology of T1D was tested directly by treating female NOD mice with agents capable of interfering with lymphangiogenesis. Administration of axitinib, a kinase inhibitor that targets VEGFR1-3 and blocks signaling of the most important growth factor of lymphangiogenesis, VEGF-C (64, 65), from week 3 to 5 delayed the onset of hyperglycemia by a period nearly equivalent to the duration of treatment (Fig. 4A). In contrast, feeding of the Prox1 pathway with dietary acetate (66) accelerated the onset of disease (Fig. 4B). A similar intervention with a neutralizing Ab against NRP2 (67), an alternative ligand coreceptor for VEGF-C (68) and expressed in the IATLSs (Supplemental Table I), delayed diabetes onset by a time equivalent to the duration of treatment.

The temporary success of all interventions suggested that neolymphangiogenesis was necessary for the initiation of pathology whereas relapse was indicative of persistent prolymphangiogenesis drivers.

Sporadic local inflammation is present in efferent blood vessels of normal islets

Most innate sensing converges on the NF-κB pathway of signaling to induce inflammation. One of the targets of NF-κB is Prox-1, the master switch of lymphangiogenesis (69). It is believed that Prox-1 expression must be induced and sustained to allow lymphatic structures to establish and persist (70). Postcapillary venous endothelial cells are the main cell type that will differentiate into lymphatic endothelial cells (50), and they appear to be where IATLSs are built. The same postcapillary venules are where inflammation is sensed in tissues and the only segment where the endothelium is fenestrated (27, 71). Therefore, the islet vasculature was examined for signs of inflammation. First, the absence or only anecdotal presence of neutrophils near islets or IATLSs (Supplemental Table I) and the absence of antimicrobial peptides such as Reg3g (72) at the same sites (Supplemental Table I) in the early stages of pathology indicated that ongoing bacterial proliferation was unlikely. In contrast, activated platelets labeled with CD41 Abs, a reliable marker of endothelial inflammation (73), were often found in vessels near islets together with CLEC2-expressing cells (one of the ligands of podoplanin) (Fig. 4C).

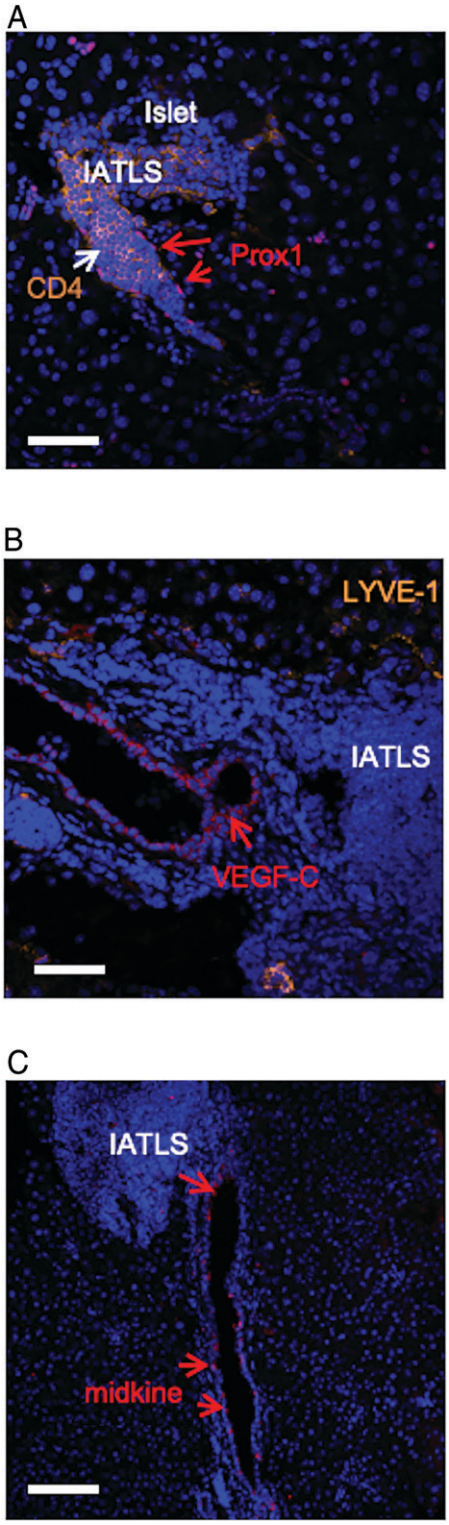

FIGURE 3. Detection of key prolymphangiogenesis molecules in the vasculature associated with IATLS. (**A–C**) Pancreases of 9-wk-old mice were stained with three of the most important molecules of lymphangiogenesis, that is, (A) Prox1, the master transcription factor, (B) VEGF-C, the growth factor, and (C) midkine, one of the essential seeding factors for lymphatic sprouts. All three were expressed by lymphatic endothelial cells associated with the IATLS. Prox1$^+$ cells were lining the outside of the IATLS itself. Scale bars, 50 μm.

The potential role of platelets in the development of the early phase of disease was directly tested with depleting anti-GP1b Abs (74). Similar to other interferences of the process of lymphangiogenesis

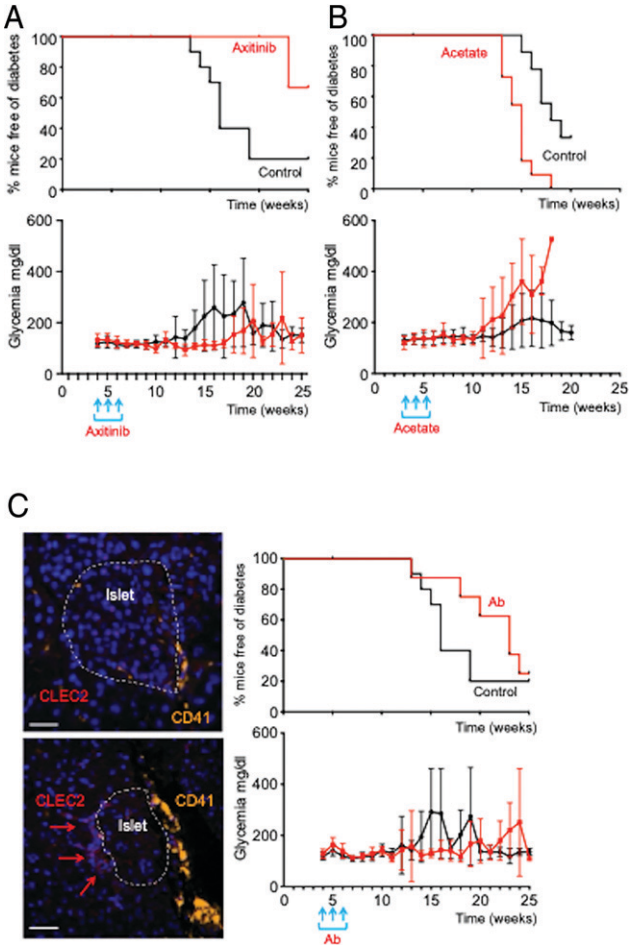

FIGURE 4. Various therapeutic interventions in young NOD mice delayed but did not prevent disease onset. (**A**) The anti-VEGFR kinase inhibitor axitinib was administered every other day for 3 wk and delayed onset by ~5 wk. At the end of study, the *p* value for survival was 0.0029, and <0.0001 for predicted mean glycemia (control 175.1 mg/dl, versus for treated mice 135.3 mg/dl). Between control and treated groups the hazard ratio is 3.961. The graph is the combination of two independent experiments (20 mice) with 5 controls and 5 axitinib-treated mice in each experiment. (**B**) The administration for 3 wk of sodium acetate to support the activity of Prox1 accelerated the disease by an equivalent period. Both survival and glycemia curves were significantly different with *p* values of 0.006 for both survival and predicted glycemia at 20 wk when the experiment was completed. Between control and treated groups the hazard ratio is 0.1481. The graph is a combination of two independent experiments with a total of 13 control mice and 15 acetate-treated animals. (**C**) Based on CD41 staining, activated platelets were detected in blood vessels associated with the islets of NOD mice. The elimination of platelets by Ab injection during 3 wk delayed onset by ~3 wk. At 25 wk, the survival difference was not significant but the predicted mean glycemia was with a *p* value of <0.0001. Between control and treated groups the hazard ratio is 1.587. The graph is the combination of two independent experiments with 10 controls and 10 Ab-treated mice in each experiment. Scale bars, 50 μm.

(Fig. 4A, 4B), this treatment when applied once a week from week 4 to 6 delayed onset by ~3 wk (Fig. 4C), suggesting a sustained role for platelets in the development of disease, as well as a persistent activation of platelets by endothelial inflammation.

Two reliable markers of inflammation, VCAM-1 and CD29 (75, 76), were examined for expression in the islet vasculature in young NOD mice. Both proteins were present on blood vessels identifiable as venules adjacent to IATLSs (Fig. 5A) and in normal tissue (Fig. 5D), whereas intraislet capillaries were negative. The absence of inflammation of the islet capillaries was confirmed by profiling single $CD45^{-}CD31^{+}MECA32^{+}$ endothelial cells from whole islets (MECA32 was expressed primarily by this population; see Supplemental Fig. 2C) with the gene array used for macrophages. Unlike macrophages, $MECA32^{+}$ capillary endothelial cells did not express measurable amounts of IL-1α or IL-1β and no or very low levels of MHC class II mRNA as seen by others (77) and no accessory molecules for Ag presentation (CD74, H-2M, cathepsins, CD80, CD86), indicating their relative quiescence.

The inflammation of the extraislet vasculature was confirmed by the presence of other markers such as NO synthase 3 (NOS3) (78), closely associated with the vasculature and the IATLSs depending on the stage of disease (Fig. 5B) and coexpressed with MHC class II molecules (Fig. 5B, 5C). Some anti-inflammatory molecules such as clusterin (79) were predominantly expressed at the periphery of islets where NOS3 was highly present (Fig. 5B).

In conclusion, inflammation of the extraislet vasculature was detected prior to T cell infiltration in every NOD mouse we examined and increased while the IATLS was built, whereas the intraislet capillaries seem to be spared.

MHC class II expression in association with islets

Increased MHC class I and de novo MHC class II expressions are good markers of inflammation in all tissues, as they report the making of two proinflammatory cytokines, IFN-γ and TNF-α. Because T1D is a CD4 T cell–mediated disease as proven by its overwhelming association with non-Aspβ57 diabetogenic MHC molecules in mice and humans (80, 81), the description of islet-associated cells expressing MHC class II molecules has been a primary focus of T1D research. Based on early reports (16, 18) and the fact that only hematopoietic cells express MHC class II constitutively, our attention was focused on the rare intraislet macrophage (82). More recently, rare cells were shown to coexpress insulin and MHC class II and were likely β cells (15, 83). In this study, the same issue was revisited by staining mouse and human pancreatic sections for MHC class II expression followed by confocal microscopy. Positive cells were found outside of the islet of both species (Fig. 5D, 5E). These MHC class II–positive cells were always associated with ER-TR7–expressing cells and close to efferent blood vessels (Fig. 5D, 5E). The initial accumulation of cells in insulitis of both species was found next to the same area and accompanied by an increase in the number of ER-TR7 MHC class II–positive cells (Fig. 5D). The nonhematopoietic nature of these cells and their increased number during disease progression were confirmed by cytometry and CD45 labeling of purified dissociated islets (see Fig. 8). The same MHC class II expression was present in nonsusceptible NOD strains such as C57BL/6 or NODβ57D (23), but at a much lower level, never exceeding >1.5%.

Lesions in human samples: mouse and human similarities

It has long been debated whether the human insulitis lesion was similar to its mouse counterpart or even existed (1, 84). In this study, we provide five unifying anatomical and pathological features between mouse and human T1D: 1) No lymphatics were found associated with normal islets in both species; in all normal samples 16 islets were visualized for LYVE-1/insulin, and none was associated with this lymphatic endothelium marker (Figs. 2A, 6A). 2) Lymphatics were associated with islets undergoing destruction as signified by the presence of $LYVE\text{-}1^{+}$ cells and vessels next to or within diseased islets of T1D patients; in nPOD T1D samples, slides stained for LYVE-1/insulin showed 16 islets that were associated with $LYVE\text{-}1^{+}$ vessels and 8 that were not (Fig. 6B, 6C). 3) As in the mouse and for human CD8 T cells (19), CD4 T cells were found outside of the islet in human T1D samples (Fig. 6D). 4) The ER-TR7 scaffolding, and associated heparan sulfate BM of the human islet, was identical to the one found in mice (Supplemental Table I). 5) Finally, and

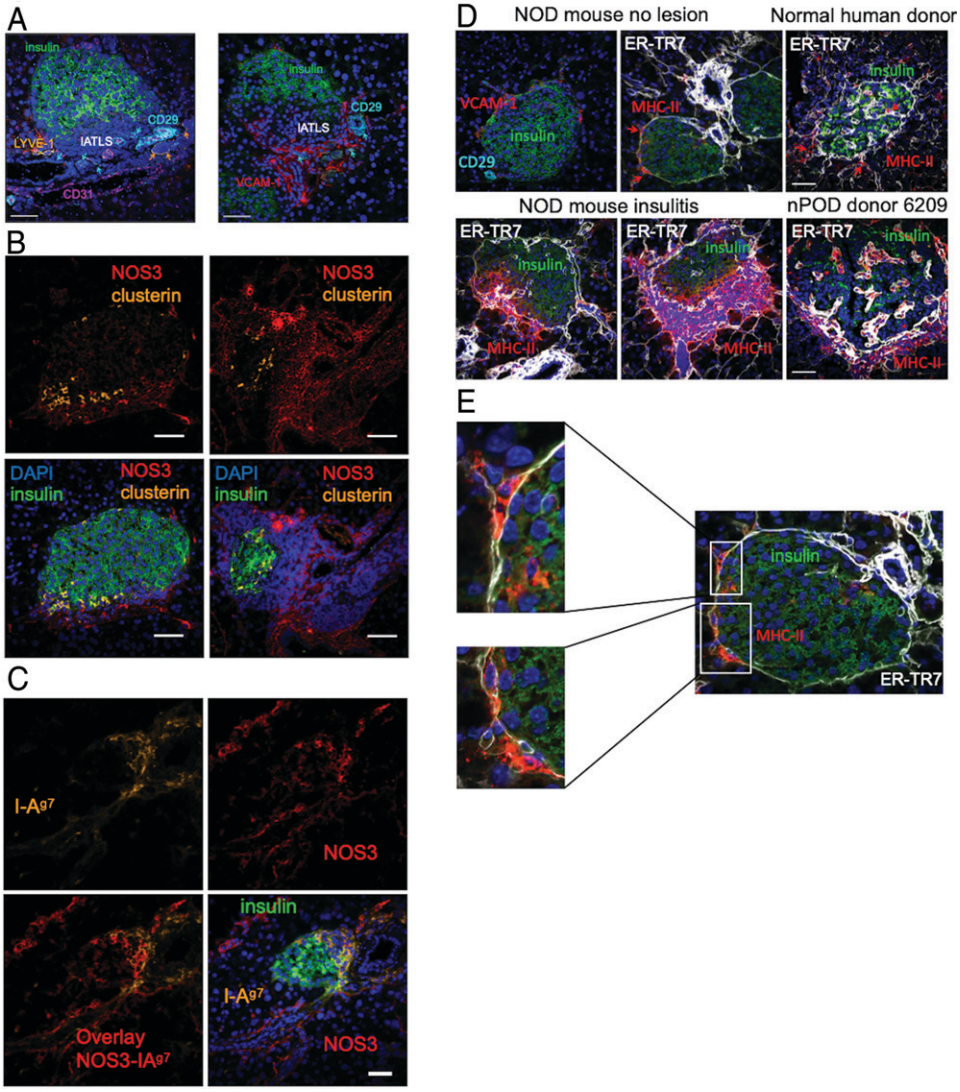

FIGURE 5. Presence of inflammatory markers in the vasculature associated with the islet and IATLS. (**A**) $CD29^+$ (left) and VCAM-1^+ (right) cells were present and intermixed with the IATLS. (**B**) High expression of NOS3 at the early (left panels) and late (right panels) phase of the IATLS development. Cells expressing clusterin were detected at the boundary islet/IATLS. (**C**) NOS3 expression colocalized with the expression of MHC class II. (**D**) $CD29^+$ and VCAM-1^+ cells were also detected in unaffected mouse islets in locations where collecting veins exited the endocrine structure and where MHC class II could be seen and was associated with the basement membrane marker ER-TR7. Human normal islets displayed a similar feature with HLA class II^+ ER-$TR7^+$ cells outside of the endocrine tissue. The number of MHC class II^+ ER-$TR7^+$ cells was greatly increased in diseased mouse and human islets. (**E**) Zoomed-in region of an unaffected NOD mouse islet showing MHC class II^+ ER-$TR7^+$ cells. Scale bars, 50 μm.

most importantly, in normal islets of both mice and humans, the dominant MHC class II–expressing cells were found outside of the islets, near the efferent blood vessels, a feature that had not yet been reported. This location was also where insulitis was initiated, as documented in mice (Fig. 2) and observed in humans (Fig. 6D).

Origin of the pancreatic inflammation? Duodenum–pancreas communication? Increasing extrailset MHC class II expression with an oral inflammatory compound

The evidence for direct communication between duodenal content and the pancreas was demonstrated years ago in an assay in which pLN-resident CD4 T cells were stimulated by gavage with an Ag (85); this has been confirmed since for bacterial components (86). In this study, we examined and confirmed with Ab staining the presence of two fundamental proinflammatory bacterial chemical entities that most likely originate from the intestinal microbiome: muramyl dipeptides (MDP) of Gram-positive bacteria (Supplemental Fig. 3), and LPS of Gram-negative bacteria. As seen in Supplemental Fig. 3, at steady state, in non-T1D susceptible strains such as the C57BL/6-I-A^{g7}, both LPS and MDP were found associated with the vasculature of the pancreas, endothelium for LPS, and perivascular cells for MDP. In NOD mice, images were nearly identical before the onset of pathology (Supplemental Fig. 3), and markedly increased for MDP at the periphery of IATLSs when pathology was detectable (Supplemental Fig. 3). The cells labeled for MDP all appeared to be expressing NOD2, the intracellular sensor for this molecule (Supplemental Fig. 3).

We confirmed in these experiments that the vasculature of the pancreas was directly exposed to a large collection of biomolecules capable of crossing the duodenal barrier, and in some cases triggering segmental inflammation. This concept was challenged in a dynamic experiment in which mice were administered poly(I:C), a known trigger or accelerator of disease (34, 87). One hundred micrograms of poly(I:C) was orally gavaged for 4–6 consecutive days to NOD mice and islet-associated MHC class II and insulin expression levels were quantified across 41 and 30 islets in five control and five treated mice, respectively. Following this course of treatment, poly(I:C) induced a robust and significant increase in MHC class II expression ($p = 0.001$) whereas insulin stain was significantly decreased in comparison with the control animals ($p = 0.006$) (Fig. 7A). A similar increase in HLA-DQ8 near islets was noted in the YES mice after the same treatment (Fig. 7B) and in the nondiabetic NODβ57D mouse (Fig. 7C). Therefore, proinflammatory compounds provided orally were capable of increasing MHC class II expression in all genetic backgrounds and to drive disease progression in T1D-prone mice.

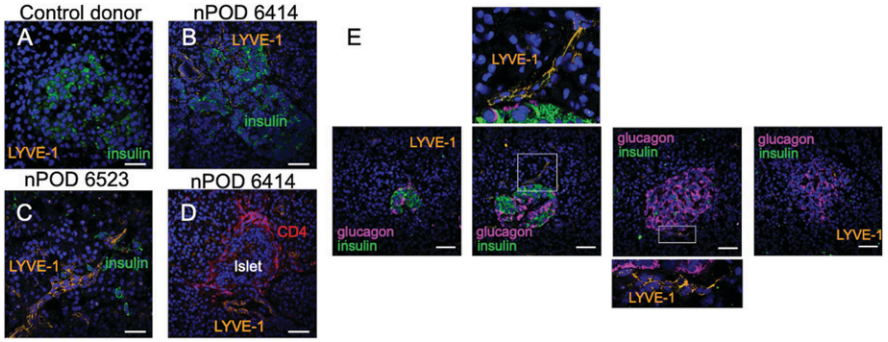

FIGURE 6. Anatomy of lymphatics in normal and diseased human pancreatic islets. (**A**) No LYVE-1 islet-associated staining was detected in tissue from normal donors. (**B** and **C**) Lymphatics were present in islets from type 1 diabetes donors. (**D**) Similar to the NOD mouse lesion, CD4 T cells accumulated on the outside of the islet and were associated to lymphatic vessels. (**E**) Based on the intensity of the insulin stain, the successive steps of the human lesion are shown in a single specimen in which, from left to right, normal islets, lymphatic-associated islets, and nearly and fully destroyed islets were found. Zoomed-in regions where LYVE-1 staining was present showed the intimate relationship between lymphatics and the outside of the islet. Scale bars, 50 μm.

Spontaneous presentation of islet Ags by CD45$^-$ MHC class II$^+$ cells

Besides their expression of MHC class II, the CD45$^-$ cells were further characterized with two classic markers of fibroblast, gp38 (podoplanin), and vascular endothelium, CD31. As shown in Fig. 8A, a large increase in MHC class II expression was seen between 6 and 10 wk, and both fibroblasts and endothelial cells were represented in this population in nearly identical numbers. The functionality of the total CD45$^-$ MHC class II$^+$ cell population was tested after enzymatic dissociation of islets and depletion of CD45$^+$ cells by two rounds of magnetic sorting. Without addition of exogenous Ag, these cells were capable of stimulating the anti-BDC2.5 T cell hybridoma BC28 whereas cells from MHC class II knockout mice could not (Fig. 8B). We concluded that this population had APC function and that its MHC class II molecules were loaded with islet Ags (Fig. 9).

Discussion

The current work is meant to understand the early mechanisms of anti-islet immunity; that is, "What are the initiating APCs expressing MHC class II and stimulating anti-islet CD4 T cells?", and "How do CD4 T cells access the islet?" Until now, our attention was focused on the intraislet macrophage (82) and the β cell itself, which might express MHC class II upon IFN-γ exposure (88). Both cells positioned the autoimmune response within the islet of Langerhans. However, little direct evidence supports these conclusions, yet: no macrophage–T cell or β cell–T cell synapse, no two-photon live imaging, and most importantly the dominant extraislet location of all T cells both in mice and humans. Nonetheless, this intraislet-centric view of the T1D lesion persisted because anti-insulin T cell priming was shown to be associated with the islet and not the pLNs (23, 24, 89), and healthy islets are devoid of lymphatics (25). Repositioning the disease initiation outside the islet implied that neolymphangiogenesis was a necessary step for the autoimmune reaction such as is seen in the attack of other immune-privileged sites such as the eye and the brain (44–46). This observation has semantic consequences; indeed, we would argue that all T1D lesions are peri-insulitis in nature, and that the term insulitis is not accurate. Appearance of insulitis could easily be given by the incidence of a single section through the islet and the cuff of peri-insulitis. In this study, we timed the islet-associated lymphangiogenesis between weeks 5 and 8 by examining the state of activation of circulating anti-insulin CD4 T cells. The importance of lymphatic circulation in the progression of T1D pathology (90, 91) was demonstrated by the

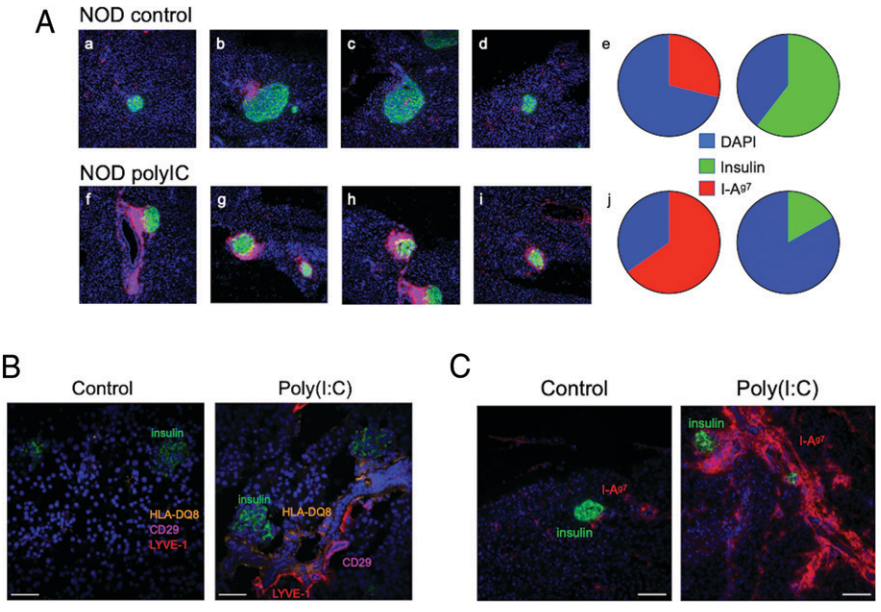

FIGURE 7. Poly(I:C) induces the expression of MHC class II in the islet-draining vasculature of NOD mice, humanized YES mice, and NODβ57 mice. (**A**) After 6 d of oral gavage, mock- and poly(I:C)-treated NOD mice were examined for insulin and MHC class II expression. Representative sections in each group are shown. The quantitation of stained areas was performed using Zen software on 41 islets from the control group and 30 from the poly(I:C)-treated group and is presented as a pie graph. The *p* values calculated with a two-tail *t* test are 0.006 for insulin and 0.001 for MHC class II. For each area, cell numbers were counted using the DAPI channel (original magnification ×20). (**B**) In YES mice, poly(I:C) administered for 4 consecutive days induced a similar expression of HLA-DQ8 associated with the vasculature of the islet. (**C**) MHC class II expression was triggered in diabetes-resistant NODβ57 mice by poly(I:C) gavage.

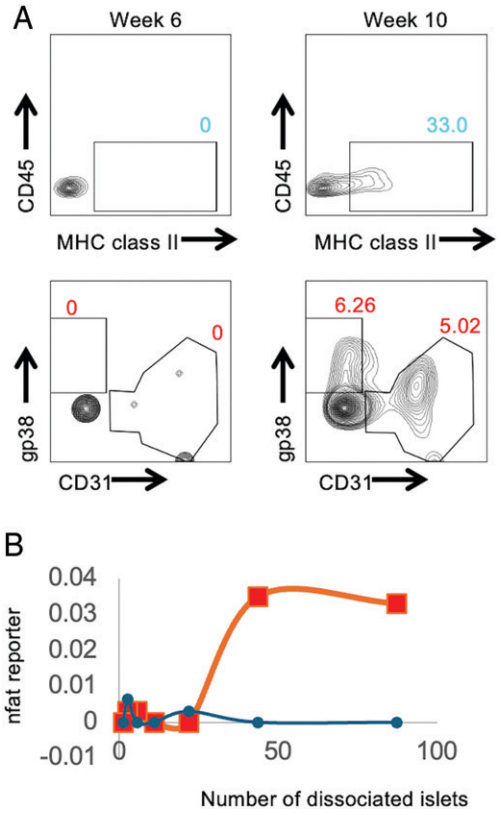

FIGURE 8. Nonhematopoietic cells that are associated with the islet express MHC class II molecules over time and spontaneously present islet Ags. (**A**) In this experiment, between 6 and 10 wk, 33% of $CD45^-$ cells became positive for MHC class II expression. This population could be qualified as a mixture of endothelial-related cells ($CD31^+$) and fibroblasts ($gp38^+$). (**B**) Islets of three 10-wk-old NOD mice were isolated and enzymatically dispersed before being depleted of $CD45^+$ cells by successive passages on anti-CD45 columns. $CD45^-$ cells were too few to be counted and were expressed as "islet equivalent." These cells were incubated in the presence of an anti-BDC2.5 T cell hybridoma, BC28, for 16 h without addition of Ag. Nfat activation was measured by flow cytometry using the violet signal of ametrine. The negative control was cells isolated from islets of MHC class II^- NOD mice using the same procedure. Both experiments were repeated with similar results.

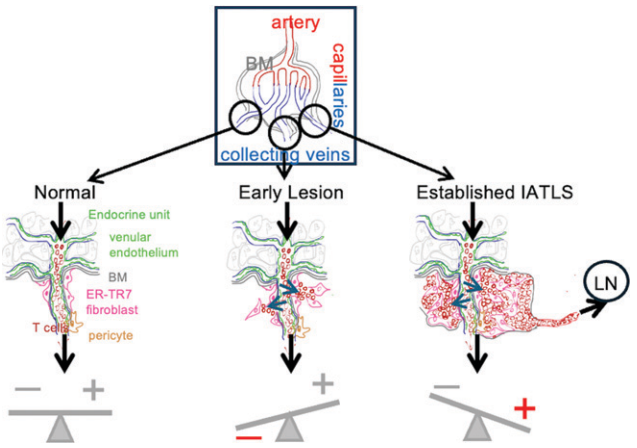

FIGURE 9. Schematic representation of the progression of disease in islets based on our observations. In the insert is a schematic representation of the islet vasculature with a single artery, followed by the capillary bed and its collapse into collecting venules. The endocrine cells are insulated from the vasculature by a double basement membrane (BM). In a normal situation in the absence of inflammation, cells from the blood flow through the islet and access the general circulation. When inflammation is sensed in the postcapillary venule, the endothelium layer promotes cell attachment and extravasation. In the early lesion, extravasated cells encounter the ER-TR7 fibroblastic cell, of which some express MHC class II. At that stage we hypothesize that negative regulation controls the state of activation of T cells. When the inflammation is sustained, the influx of more professional APCs in the lesion, including macrophages, B cells, and dendritic cells, overcomes the negative regulation provided by the fibroblasts and leads to full activation. The balance shown under each of the stages summarizes the outcome of each situation with respect to CD4 T cell activation.

efficacy of antilymphangiogenesis interventions. However, each of those was short-lived and suggested that persistent prolymphangiogenic cues were present. The same picture is slowly emerging in humans with the recent description of IATLS in nPOD samples (92). Moreover, in a direct translational study we have shown that in at-risk populations and patients, the circulation of activated anti-insulin CD4 T cells was diagnostic of disease progression (5).

As for the origin of lymphangiogenesis, local vascular inflammation is the most likely driver, and segments of the proximal part of the postcapillary venule expressed activation markers, for example, CD29, VCAM-1, NOS3, and MHC class II. The causes of this inflammation remain unclear, but at steady state biomolecules ingested or produced locally by the intestinal microbiome such as LPS or MDP were detected in association with blood vessels. Moreover, the receptor for MDP, NOD2, was expressed in the same location as MDP. Finally, orally administered proinflammatory molecule such as poly(I:C) increased the local vascular inflammation and the expression of MHC class II molecules. The transport of biomolecules from the duodenum to the pancreas (85), the role of the loss of the gut barrier in increasing the incidence of T1D (93, 94), and the importance of MDP sensing by NOD2 for the induction of the streptozotocin effects (86) all argue for the same model, that is, duodenum–pancreas transport controls vascular inflammation and T1D.

Our study refocuses T1D pathology to the islet postcapillary venule, a site where inflammation is sensed in every organ and associated with the anatomy of its interendothelial junctions that allow intercytosis (27, 95, 96). This part of the vasculature is where MHC class II^+ cells are found in intact islets and where the insulitis is built. These nonhematopoietic MHC class II–expressing cells are juxtaposed to the CD4 T cells in the IATLS and spontaneously present islet Ags ex vivo. The control of their number and MHC class II expression by short-term gavage with poly(I:C) is one additional reason that suggests their importance in the initiation of disease. By their location, these cells are also ideally suited to pick up at the time of insulin secretion β cell crinosomes that contain the byproducts of insulin maturation and unique peptides such as $InsB_{12–20}$ (97).

The model that we propose is depicted in Fig. 9: inflammation triggers blood cell extravasation, local production of IFNs induces MHC class I and II expression on the perivascular cells, these nonhematopoietic cells activate CD4 T cells, lymphangiogenic factors are produced, more immune cells are recruited, CD4 T cells become fully activated, and cytokines and CD8 contribute to β cell death.

The full characterization of the $CD45^-$ MHC class II^+ cells that we introduce in this study should shed important clues on the early phase of T1D pathology.

Acknowledgements

We are grateful to the Network for Pancreatic Organ Donors (nPOD), and to the donors and families of donors of the nPOD program for supporting our science. We thank Dr. Wolfram Ruff for providing advice and the antiplatelet Abs. We thank Dr. Louis Gioia for writing the first R scripts that allowed us to analyze gene expression data. We are also grateful to Brian Monteverde

and Brian Seegers of the Flow Cytometry Core at Scripps Research for spending late evenings running our samples, and Kathryn Spencer and Scott Henderson of the Microscopy Core for supporting us.

Disclosures

The authors have no financial conflicts of interest.

References

1. In't Veld, P. 2011. Insulitis in human type 1 diabetes: the quest for an elusive lesion. *Islets* 3: 131–138.
2. In't Veld, P. 2014. Insulitis in human type 1 diabetes: a comparison between patients and animal models. *Semin. Immunopathol*. 36: 569–579.
3. Koskinen, M. K., O. Helminen, J. Matomäki, S. Aspholm, J. Mykkänen, M. Mäkinen, V. Simell, M. Vähä-Mäkilä, T. Simell, J. Ilonen, et al. 2016. Reduced β-cell function in early preclinical type 1 diabetes. *Eur. J. Endocrinol*. 174: 251–259.
4. Knip, M. 2002. Natural course of preclinical type 1 diabetes. *Horm. Res*. 57 (Suppl. 1): 6–11.
5. Sharma, S., X. Tan, J. Boyer, D. Clarke, A. Costanzo, B. Abe, L. Kain, M. Holt, A. Armstrong, M. Rihanek, et al. 2023. Measuring anti-islet autoimmunity in mouse and human by profiling peripheral blood antigen-specific CD4 T cells. *Sci. Transl. Med*. 15: eade3614.
6. Makhlouf, L., S. T. Grey, V. Dong, E. Csizmadia, M. B. Arvelo, H. Auchincloss, Jr., C. Ferran, and M. H. Sayegh. 2004. Depleting anti-CD4 monoclonal antibody cures new-onset diabetes, prevents recurrent autoimmune diabetes, and delays allograft rejection in nonobese diabetic mice. *Transplantation* 77: 990–997.
7. Hamilton-Williams, E. E., S. E. Palmer, B. Charlton, and R. M. Slattery. 2003. Beta cell MHC class I is a late requirement for diabetes. *Proc. Natl. Acad. Sci. USA* 100: 6688–6693.
8. Lambelet, M., L. F. Terra, M. Fukaya, K. Meyerovich, L. Labriola, A. K. Cardozo, and F. Allagnat. 2018. Dysfunctional autophagy following exposure to pro-inflammatory cytokines contributes to pancreatic β-cell apoptosis. *Cell Death Dis*. 9: 96.
9. Roep, B. O., and M. Peakman. 2012. Antigen targets of type 1 diabetes autoimmunity. *Cold Spring Harb. Perspect. Med*. 2: a007781.
10. Delong, T., T. A. Wiles, R. L. Baker, B. Bradley, G. Barbour, R. Reisdorph, M. Armstrong, R. L. Powell, N. Reisdorph, N. Kumar, et al. 2016. Pathogenic CD4 T cells in type 1 diabetes recognize epitopes formed by peptide fusion. *Science* 351: 711–714.
11. Richardson, S. J., T. Rodriguez-Calvo, I. C. Gerling, C. E. Mathews, J. S. Kaddis, M. A. Russell, M. Zeissler, P. Leete, L. Krogvold, K. Dahl-Jørgensen, et al. 2016. Islet cell hyperexpression of HLA class I antigens: a defining feature in type 1 diabetes. *Diabetologia* 59: 2448–2458.
12. James, E. A., A. V. Joglekar, A. K. Linnemann, H. A. Russ, and S. C. Kent. 2023. The beta cell-immune cell interface in type 1 diabetes (T1D). *Mol. Metab.* 78: 101809.
13. Zhao, Y., N. A. Scott, H. S. Quah, B. Krishnamurthy, F. Bond, T. Loudovaris, S. I. Mannering, T. W. Kay, and H. E. Thomas. 2015. Mouse pancreatic β cells express MHC class II and stimulate $CD4^+$ T cells to proliferate. *Eur. J. Immunol*. 45: 2494–2503.
14. Foulis, A. K., and M. A. Farquharson. 1986. Aberrant expression of HLA-DR antigens by insulin-containing β-cells in recent-onset type I diabetes mellitus. *Diabetes* 35: 1215–1224.
15. Russell, M. A., S. D. Redick, D. M. Blodgett, S. J. Richardson, P. Leete, L. Krogvold, K. Dahl-Jørgensen, R. Bottino, M. Brissova, J. M. Spaeth, et al. 2019. HLA class II antigen processing and presentation pathway components demonstrated by transcriptome and protein analyses of islet β-cells from donors with type 1 diabetes. *Diabetes* 68: 988–1001.
16. McInerney, M. F., S. Rath, and C. A. Janeway, Jr. 1991. Exclusive expression of MHC class II proteins on $CD45^+$ cells in pancreatic islets of NOD mice. *Diabetes* 40: 648–651.
17. Carrero, J. A., D. P. McCarthy, S. T. Ferris, X. Wan, H. Hu, B. H. Zinselmeyer, A. N. Vomund, and E. R. Unanue. 2017. Resident macrophages of pancreatic islets have a seminal role in the initiation of autoimmune diabetes of NOD mice. *Proc. Natl. Acad. Sci. USA* 114: E10418–E10427.
18. Bottazzo, G. F., B. M. Dean, J. M. McNally, E. H. MacKay, P. G. Swift, and D. R. Gamble. 1985. In situ characterization of autoimmune phenomena and expression of HLA molecules in the pancreas in diabetic insulitis. *N Engl. J. Med.* 313: 353–360.
19. Coppieters, K. T., F. Dotta, N. Amirian, P. D. Campbell, T. W. Kay, M. A. Atkinson, B. O. Roep, and M. G. von Herrath. 2012. Demonstration of islet-autoreactive CD8 T cells in insulitic lesions from recent onset and long-term type 1 diabetes patients. *J. Exp. Med*. 209: 51–60.
20. Campbell-Thompson, M. L., M. A. Atkinson, A. E. Butler, N. M. Chapman, G. Frisk, R. Gianani, B. N. Giepmans, M. G. von Herrath, H. Hyöty, T. W. Kay, et al. 2013. The diagnosis of insulitis in human type 1 diabetes. *Diabetologia* 56: 2541–2543.
21. Kuric, E., P. Seiron, L. Krogvold, B. Edwin, T. Buanes, K. F. Hanssen, O. Skog, K. Dahl-Jørgensen, and O. Korsgren. 2017. Demonstration of tissue resident memory CD8 T cells in insulitic lesions in adult patients with recent-onset type 1 diabetes. *Am. J. Pathol*. 187: 581–588.
22. Höglund, P., J. Mintern, C. Waltzinger, W. Heath, C. Benoist, and D. Mathis. 1999. Initiation of autoimmune diabetes by developmentally regulated presentation of islet cell antigens in the pancreatic lymph nodes. *J. Exp. Med*. 189: 331–339.
23. Gioia, L., M. Holt, A. Costanzo, S. Sharma, B. Abe, L. Kain, M. Nakayama, X. Wan, A. Su, C. Mathews, et al. 2019. Position β57 of $I\text{-}A^{g7}$ controls early anti-insulin responses in NOD mice, linking an MHC susceptibility allele to type 1 diabetes onset. *Sci. Immunol*. 4:
24. Mohan, J. F., B. Calderon, M. S. Anderson, and E. R. Unanue. 2013. Pathogenic $CD4^+$ T cells recognizing an unstable peptide of insulin are directly recruited into islets bypassing local lymph nodes. *J. Exp. Med*. 210: 2403–2414.
25. Korsgren, E., and O. Korsgren. 2016. An apparent deficiency of lymphatic capillaries in the islets of Langerhans in the human pancreas. *Diabetes* 65: 1004–1008.
26. Korpos, E., N. Kadri, R. Kappelhoff, J. Wegner, C. M. Overall, E. Weber, D. Holmberg, S. Cardell, and L. Sorokin. 2013. The peri-islet basement membrane, a barrier to infiltrating leukocytes in type 1 diabetes in mouse and human. *Diabetes* 62: 531–542.
27. Palade, G. E., M. Simionescu, and N. Simionescu. 1979. Structural aspects of the permeability of the microvascular endothelium. *Acta Physiol. Scand. Suppl*. 463: 11–32.
28. Bonner-Weir, S., and L. Orci. 1982. New perspectives on the microvasculature of the islets of Langerhans in the rat. *Diabetes* 31: 883–889.
29. Dybala, M. P., A. Kuznetsov, M. Motobu, B. K. Hendren-Santiago, L. H. Philipson, A. V. Chervonsky, and M. Hara. 2020. Integrated pancreatic blood flow: bidirectional microcirculation between endocrine and exocrine pancreas. *Diabetes* 69: 1439–1450.
30. Dybala, M. P., and M. Hara. 2019. Heterogeneity of the human pancreatic islet. *Diabetes* 68: 1230–1239.
31. Kim, H., R. P. Kataru, and G. Y. Koh. 2014. Inflammation-associated lymphangiogenesis: a double-edged sword? *J. Clin. Invest*. 124: 936–942.
32. Tammela, T., and K. Alitalo. 2010. Lymphangiogenesis: molecular mechanisms and future promise. *Cell* 140: 460–476.
33. Mounzer, R. H., O. S. Svendsen, P. Baluk, C. M. Bergman, T. P. Padera, H. Wiig, R. K. Jain, D. M. McDonald, and N. H. Ruddle. 2010. Lymphotoxin-alpha contributes to lymphangiogenesis. *Blood* 116: 2173–2182.
34. Luce, S., S. Guinoiseau, A. Gadault, F. Letourneur, B. Blondeau, P. Nitschke, E. Pasmant, M. Vidaud, F. Lemonnier, and C. Boitard. 2018. Humanized mouse model to study type 1 diabetes. *Diabetes* 67: 1816–1829.
35. Li, D. S., Y. H. Yuan, H. J. Tu, Q. L. Liang, and L. J. Dai. 2009. A protocol for islet isolation from mouse pancreas. *Nat. Protoc*. 4: 1649–1652.
36. Holt, M., A. Costanzo, L. Gioia, B. Abe, A. I. Su, and L. Teyton. 2018. Gene profiling and T cell receptor sequencing from antigen-specific CD4 T cells. *Methods Mol. Biol.* 1712: 217–238.
37. Polonskaya, Z., S. Deng, A. Sarkar, L. Kain, M. Comellas-Aragones, C. S. McKay, K. Kaczanowska, M. Holt, R. McBride, V. Palomo, et al. 2017. T cells control the generation of nanomolar-affinity anti-glycan antibodies. *J. Clin. Invest*. 127: 1491–1504.
38. Cesmebasi, A., J. Malefant, S. D. Patel, M. Du Plessis, S. Renna, R. S. Tubbs, and M. Loukas. 2015. The surgical anatomy of the lymphatic system of the pancreas. *Clin. Anat*. 28: 527–537.
39. O'Morchoe, C. C. 1997. Lymphatic system of the pancreas. *Microsc. Res. Tech*. 37: 456–477.
40. Mullen, Y. 2017. Development of the nonobese diabetic mouse and contribution of animal models for understanding type 1 diabetes. *Pancreas* 46: 455–466.
41. Plesner, A., J. T. Ten Holder, and C. B. Verchere. 2014. Islet remodeling in female mice with spontaneous autoimmune and streptozotocin-induced diabetes. *PLoS One* 9: e102843.
42. Haskins, K., and M. McDuffie. 1990. Acceleration of diabetes in young NOD mice with a $CD4^+$ islet-specific T cell clone. 249: 1433–1436.
43. Trudeau, J. D., C. Kelly-Smith, C. B. Verchere, J. F. Elliott, J. P. Dutz, D. T. Finegood, P. Santamaria, and R. Tan. 2003. Prediction of spontaneous autoimmune diabetes in NOD mice by quantification of autoreactive T cells in peripheral blood. *J. Clin. Invest.* 111: 217–223.
44. Kielczewski, J. L., R. Horai, Y. Jittayasothorn, C. C. Chan, and R. R. Caspi. 2016. Tertiary lymphoid tissue forms in retinas of mice with spontaneous autoimmune uveitis and has consequences on visual function. *J. Immunol*. 196: 1013–1025.
45. Prineas, J. W. 1979. Multiple sclerosis: presence of lymphatic capillaries and lymphoid tissue in the brain and spinal cord. *Science* 203: 1123–1125.
46. Mitsdoerffer, M., and A. Peters. 2016. Tertiary lymphoid organs in central nervous system autoimmunity. *Front. Immunol*. 7: 451.
47. Neyt, K., F. Perros, C. H. GeurtsvanKessel, H. Hammad, and B. N. Lambrecht. 2012. Tertiary lymphoid organs in infection and autoimmunity. *Trends Immunol*. 33: 297–305.
48. Kerjaschki, D. 2005. The crucial role of macrophages in lymphangiogenesis. *J. Clin. Invest*. 115: 2316–2319.
49. Osada, M., O. Inoue, G. Ding, T. Shirai, H. Ichise, K. Hirayama, K. Takano, Y. Yatomi, M. Hirashima, H. Fujii, et al. 2012. Platelet activation receptor CLEC-2 regulates blood/lymphatic vessel separation by inhibiting proliferation, migration, and tube formation of lymphatic endothelial cells. *J. Biol. Chem*. 287: 22241–22252.
50. Zheng, W., A. Aspelund, and K. Alitalo. 2014. Lymphangiogenic factors, mechanisms, and applications. *J. Clin. Invest*. 124: 878–887.
51. Katakai, T., T. Hara, M. Sugai, H. Gonda, and A. Shimizu. 2004. Lymph node fibroblastic reticular cells construct the stromal reticulum via contact with lymphocytes. *J. Exp. Med*. 200: 783–795.
52. Burrell, B. E., K. J. Warren, Y. Nakayama, D. Iwami, C. C. Brinkman, and J. S. Bromberg. 2015. Lymph node stromal fiber ER-TR7 modulates $CD4^+$ T cell lymph node trafficking and transplant tolerance. *Transplantation* 99: 1119–1125.
53. Schiavinato, A., M. Przyklenk, B. Kobbe, M. Paulsson, and R. Wagener. 2021. Collagen type VI is the antigen recognized by the ER-TR7 antibody. *Eur. J. Immunol*. 51: 2345–2347.
54. Irving-Rodgers, H. F., A. F. Ziolkowski, C. R. Parish, Y. Sado, Y. Ninomiya, C. J. Simeonovic, and R. J. Rodgers. 2008. Molecular composition of the peri-

islet basement membrane in NOD mice: a barrier against destructive insulitis. *Diabetologia* 51: 1680–1688.
55. Vaahtomeri, K., S. Karaman, T. Mäkinen, and K. Alitalo. 2017. Lymphangiogenesis guidance by paracrine and pericellular factors. *Genes Dev*. 31: 1615–1634.
56. Olmeda, D., D. Cerezo-Wallis, E. Riveiro-Falkenbach, P. C. Pennacchi, M. Contreras-Alcalde, N. Ibarz, M. Cifdaloz, X. Catena, T. G. Calvo, E. Cañón, et al. 2017. Whole-body imaging of lymphovascular niches identifies pre-metastatic roles of midkine. *Nature* 546: 676–680.
57. Ager, A. 2017. High endothelial venules and other blood vessels: critical regulators of lymphoid organ development and function. *Front. Immunol*. 8: 45.
58. Ji, R. C. 2012. Macrophages are important mediators of either tumor- or inflammation-induced lymphangiogenesis. *Cell. Mol. Life Sci*. 69: 897–914.
59. Ferris, S. T., P. N. Zakharov, X. Wan, B. Calderon, M. N. Artyomov, E. R. Unanue, and J. A. Carrero. 2017. The islet-resident macrophage is in an inflammatory state and senses microbial products in blood. *J. Exp. Med*. 214: 2369–2385.
60. Karlsen, T. V., T. Reikvam, A. Tofteberg, E. Nikpey, T. Skogstrand, M. Wagner, O. Tenstad, and H. Wiig. 2017. Lymphangiogenesis facilitates initial lymph formation and enhances the dendritic cell mobilizing chemokine CCL21 without affecting migration. *Arterioscler. Thromb. Vasc. Biol*. 37: 2128–2135.
61. Fujimoto, N., Y. He, M. D'Addio, C. Tacconi, M. Detmar, and L. C. Dieterich. 2020. Single-cell mapping reveals new markers and functions of lymphatic endothelial cells in lymph nodes. *PLoS Biol*. 18: e3000704.
62. Ochiai, E., Q. Sa, M. Brogli, T. Kudo, X. Wang, J. P. Dubey, and Y. Suzuki. 2015. CXCL9 is important for recruiting immune T cells into the brain and inducing an accumulation of the T cells to the areas of tachyzoite proliferation to prevent reactivation of chronic cerebral infection with Toxoplasma gondii. *Am. J. Pathol*. 185: 314–324.
63. Allende, M. L., J. L. Dreier, S. Mandala, and R. L. Proia. 2004. Expression of the sphingosine 1-phosphate receptor, S1P1, on T-cells controls thymic emigration. *J. Biol. Chem*. 279: 15396–15401.
64. Nihei, M., T. Okazaki, S. Ebihara, M. Kobayashi, K. Niu, P. Gui, T. Tamai, T. Nukiwa, M. Yamaya, T. Kikuchi, et al. 2015. Chronic inflammation, lymphangiogenesis, and effect of an anti-VEGFR therapy in a mouse model and in human patients with aspiration pneumonia. *J. Pathol*. 235: 632–645.
65. Wang, C., and M. Chu. 2021. Advances in drugs targeting lymphangiogenesis for preventing tumor progression and metastasis. *Front. Oncol*. 11: 783309.
66. Wong, B. W., X. Wang, A. Zecchin, B. Thienpont, I. Cornelissen, J. Kalucka, M. García-Caballero, R. Missiaen, H. Huang, U. Brüning, et al. 2017. The role of fatty acid beta-oxidation in lymphangiogenesis. *Nature* 542: 49–54.
67. Caunt, M., J. Mak, W. C. Liang, S. Stawicki, Q. Pan, R. K. Tong, J. Kowalski, C. Ho, H. B. Reslan, J. Ross, et al. 2008. Blocking neuropilin-2 function inhibits tumor cell metastasis. *Cancer Cell*. 13: 331–342.
68. Wang, J., Y. Huang, J. Zhang, B. Xing, W. Xuan, H. Wang, H. Huang, J. Yang, and J. Tang. 2018. NRP-2 in tumor lymphangiogenesis and lymphatic metastasis. *Cancer Lett*. 418: 176–184.
69. Flister, M. J., A. Wilber, K. L. Hall, C. Iwata, K. Miyazono, R. E. Nisato, M. S. Pepper, D. C. Zawieja, and S. Ran. 2010. Inflammation induces lymphangiogenesis through up-regulation of VEGFR-3 mediated by NF-κB and Prox1. *Blood* 115: 418–429.
70. Alitalo, K., T. Tammela, and T. V. Petrova. 2005. Lymphangiogenesis in development and human disease. *Nature* 438: 946–953.
71. Yang, X. D., N. Karin, R. Tisch, L. Steinman, and H. O. McDevitt. 1993. Inhibition of insulitis and prevention of diabetes in nonobese diabetic mice by blocking L-selectin and very late antigen 4 adhesion receptors. *Proc. Natl. Acad. Sci. USA* 90: 10494–10498.
72. Shin, J. H., and R. J. Seeley. 2019. Reg3 proteins as gut hormones? *Endocrinology* 160: 1506–1514.
73. Koupenova, M., L. Clancy, H. A. Corkrey, and J. E. Freedman. 2018. Circulating platelets as mediators of immunity, inflammation, and thrombosis. *Circ. Res*. 122: 337–351.
74. Yokota, N., A. Zarpellon, S. Chakrabarty, V. Y. Bogdanov, A. Gruber, F. J. Castellino, N. Mackman, L. G. Ellies, H. Weiler, Z. M. Ruggeri, and W. Ruf. 2014. Contributions of thrombin targets to tissue factor-dependent metastasis in hyperthrombotic mice. *J. Thromb. Haemost*. 12: 71–81.
75. Krieglstein, C. F., and D. N. Granger. 2001. Adhesion molecules and their role in vascular disease. *Am. J. Hypertens.* 14: 44S–54S.
76. Calderon, B., J. A. Carrero, M. J. Miller, and E. R. Unanue. 2011. Entry of diabetogenic T cells into islets induces changes that lead to amplification of the cellular response. *Proc. Natl. Acad. Sci. USA* 108: 1567–1572.
77. Scott, N. A., Y. Zhao, B. Krishnamurthy, S. I. Mannering, T. W. H. Kay, and H. E. Thomas. 2018. IFNγ-induced MHC class II expression on islet endothelial cells is an early marker of insulitis but is not required for diabetogenic $CD4^+$ T cell migration. *Front. Immunol*. 9: 2800.
78. Pautz, A., H. Li, and H. Kleinert. 2021. Regulation of NOS expression in vascular diseases. *Front. Biosci. (Landmark Ed.)* 26: 85–101.
79. De Miguel, Z., N. Khoury, M. J. Betley, B. Lehallier, D. Willoughby, N. Olsson, A. C. Yang, O. Hahn, N. Lu, R. T. Vest, et al. 2021. Exercise plasma boosts memory and dampens brain inflammation via clusterin. *Nature* 600: 494–499.
80. Todd, J. A., J. I. Bell, and H. O. McDevitt. 1987. HLA-DQβ gene contributes to susceptibility and resistance to insulin-dependent diabetes mellitus. *Nature* 329: 599–604.
81. Hu, X., A. J. Deutsch, T. L. Lenz, S. Onengut-Gumuscu, B. Han, W. M. Chen, J. M. Howson, J. A. Todd, P. I. de Bakker, S. S. Rich, and S. Raychaudhuri. 2015. Additive and interaction effects at three amino acid positions in HLA-DQ and HLA-DR molecules drive type 1 diabetes risk. *Nat. Genet*. 47: 898–905.
82. Calderon, B., A. Suri, M. J. Miller, and E. R. Unanue. 2008. Dendritic cells in islets of Langerhans constitutively present β cell-derived peptides bound to their class II MHC molecules. *Proc. Natl. Acad. Sci. USA* 105: 6121–6126.
83. Quesada-Masachs, E., S. Zilberman, S. Rajendran, T. Chu, S. McArdle, W. B. Kiosses, J. M. Lee, B. Yesildag, M. A. Benkahla, A. Pawlowska, et al. 2022. Upregulation of HLA class II in pancreatic beta cells from organ donors with type 1 diabetes. *Diabetologia* 65: 387–401.
84. In't Veld, P. 2015. Rodent versus human insulitis: why the huge disconnect? *Curr. Opin. Endocrinol. Diabetes Obes*. 22: 86–90.
85. Turley, S. J., J. W. Lee, N. Dutton-Swain, D. Mathis, and C. Benoist. 2005. Endocrine self and gut non-self intersect in the pancreatic lymph nodes. *Proc. Natl. Acad. Sci. USA* 102: 17729–17733.
86. Costa, F. R., M. C. Françozo, G. G. de Oliveira, A. Ignacio, A. Castoldi, D. S. Zamboni, S. G. Ramos, N. O. Câmara, M. R. de Zoete, N. W. Palm, et al. 2016. Gut microbiota translocation to the pancreatic lymph nodes triggers NOD2 activation and contributes to T1D onset. *J. Exp. Med*. 213: 1223–1239.
87. Moriyama, H., L. Wen, N. Abiru, E. Liu, L. Yu, D. Miao, R. Gianani, F. S. Wong, and G. S. Eisenbarth. 2002. Induction and acceleration of insulitis/diabetes in mice with a viral mimic (polyinosinic-polycytidylic acid) and an insulin self-peptide. *Proc. Natl. Acad. Sci. USA* 99: 5539–5544.
88. Pujol-Borrell, R., I. Todd, M. Doshi, G. F. Bottazzo, R. Sutton, D. Gray, G. R. Adolf, and M. Feldmann. 1987. HLA class II induction in human islet cells by interferon-γ plus tumour necrosis factor or lymphotoxin. *Nature* 326: 304–306.
89. Lee, Y., R. K. Chin, P. Christiansen, Y. Sun, A. V. Tumanov, J. Wang, A. V. Chervonsky, and Y. X. Fu. 2006. Recruitment and activation of naive T cells in the islets by lymphotoxin β receptor-dependent tertiary lymphoid structure. *Immunity* 25: 499–509.
90. Yin, N., N. Zhang, G. Lal, J. Xu, M. Yan, Y. Ding, and J. S. Bromberg. 2011. Lymphangiogenesis is required for pancreatic islet inflammation and diabetes. *PLoS One* 6: e28023.
91. Levisetti, M. G., A. Suri, K. Frederick, and E. R. Unanue. 2004. Absence of lymph nodes in *NOD* mice treated with lymphotoxin-β receptor immunoglobulin protects from diabetes. *Diabetes* 53: 3115–3119.
92. Korpos, É., N. Kadri, S. Loismann, C. R. Findeisen, F. Arfuso, G. W. Burke, S. J. Richardson, N. G. Morgan, M. Bogdani, A. Pugliese, and L. Sorokin. 2021. Identification and characterisation of tertiary lymphoid organs in human type 1 diabetes. *Diabetologia* 64: 1626–1641.
93. Sorini, C., I. Cosorich, M. Lo Conte, L. De Giorgi, F. Facciotti, R. Luciano, M. Rocchi, R. Ferrarese, F. Sanvito, F. Canducci, and M. Falcone. 2019. Loss of gut barrier integrity triggers activation of islet-reactive T cells and autoimmune diabetes. *Proc. Natl. Acad. Sci. USA* 116: 15140–15149.
94. Mønsted, M. Ø., N. D. Falck, K. Pedersen, K. Buschard, L. J. Holm, and M. Haupt-Jorgensen. 2021. Intestinal permeability in type 1 diabetes: an updated comprehensive overview. *J. Autoimmun*. 122: 102674.
95. Granger, D. N., and E. Senchenkova. 2010. *Inflammation and the Microcirculation.* Mogan & Claypool Life Sciences, San Rafael, CA.
96. Pober, J. S., and W. C. Sessa. 2014. Inflammation and the blood microvascular system. *Cold Spring Harb. Perspect. Biol*. 7: a016345.
97. Wan, X., B. H. Zinselmeyer, P. N. Zakharov, A. N. Vomund, R. Taniguchi, L. Santambrogio, M. S. Anderson, C. F. Lichti, and E. R. Unanue. 2018. Pancreatic islets communicate with lymphoid tissues via exocytosis of insulin peptides. *Nature.* 560: 107–111.